



## Microwave-assisted transesterification of waste cooking oil using zinc ferrite catalyst for biodiesel production

Taeke Tiiso, Upare Vishal Baburao & Anjana P Anantharaman\*

Department of Chemical Engineering, National Institute of Technology Warangal, 506004, Telangana, India

\*E-mail: anjanapa@nitw.ac.in

Received 25 January 2024; accepted 26 April 2024

Spinel nanomaterial of  $ZnFe_2O_4$  has been successfully synthesised and its high crystallinity is confirmed by x-ray diffraction analysis in the  $Fd\bar{3}m$  space group with crystallite size of around 37.96 nm. The agglomerated nature of the sample is confirmed through SEM analysis and compositional analysis using EDS. The maximum yield of 94.66% biodiesel is obtained at 15 min, 50°C temperature, 6 weight % catalyst, and 6:1 ethanol: oil conditions. The FTIR analysis and  $^1H$ -NMR analysis of waste cooking oil and biodiesel of different yields confirm the different functional groups exist in the sample and the biodiesel. The physio-chemical properties of the biodiesel match well with the literature values. The reusability of the  $ZnFe_2O_4$  confirms the yield of 80.9% after 3 cycles under the same reaction conditions.

**Keywords:** Biodiesel, Microwave-assisted method, Transesterification, Waste cooking oil, Zinc ferrite spinel

### Introduction

The Organization of the Petroleum Exporting Countries (OPEC) reports that by 2040, the demand for fuel oil will be around 109.4 million barrels/day, and diesel fuel will be 5.7 million barrels per day<sup>1</sup>. By 2050, fossil resource availability will drop tremendously due to growing demands and the dependence of economic expansion on energy<sup>2</sup>. Biofuels derived from renewable biomass sources are promising alternative fuels due to the benefits of biodegradability, non-toxicity, lower greenhouse gas emissions, and sustainable supply. Biodiesel, the fatty acid methyl or ethyl ester, is widely developed through transesterification reactions from triglycerides in oil. Biodiesel reduces greenhouse gases by 86%, particulate matter by 47%, and hydrocarbons by 67%. Similar physiochemical characteristics of biodiesel and fossil fuel assure ready usage in diesel engines with ease of storage and transportation due to higher flash points<sup>3</sup>.

The generally used feedstock of triglycerides for biodiesel production includes non-edible oils, including Karanja oil, and rubber seed oil; edible oil like palm oil, sunflower oil, and coconut oil; animal fat like chicken fat, beef tallow; and waste cooking oil (WCO)<sup>4</sup>. Using edible oil for biodiesel production has adverse effects on food resources. WCO as feedstock for biodiesel simultaneously resolves the waste disposal problem and benefits the economy. Around

23 million MT of cooking oil is consumed in India annually, of which 3 million MT can be recovered and reused. Hong *et al.*<sup>5</sup> studied WCO as feedstock for microwave-assisted transesterification reaction of biodiesel production with 98.2 % FAME content, ~41 MJ/kg higher heating value, and an acid value of 2.5 mg KOH/g oil<sup>5</sup>. A study on biodiesel production from WCO using *M. malleus* shell-derived CaO catalyst by Niju *et al.*<sup>6</sup> reports a 93.81 % conversion of biodiesel under optimised reaction parameters.

Short-chain alcohols like methanol, ethanol, and butanol are generally employed for the transesterification reactions. Ethanol has higher oil solubility, so it is chosen as an extraction solvent. The biodiesel produced using ethanol has a higher cetane number due to the formation of ethyl esters as a product having additional carbon compared to methyl esters formed while using methanol. Moreover, ethanol can be easily produced from agricultural sources<sup>7</sup>. The presence of catalyst is essential for the reaction to proceed. Homogeneous catalysts generally adopted for transesterification reactions include acid and strong base catalysts. Difficulty in catalyst separation and formation of soaps and alkali ion contamination in oil limits their application<sup>8</sup>. Alternatively, heterogeneous catalysts generally used include acidic metallic oxides, enzymatic catalysts, or alkali metal oxides<sup>9,10</sup>. Recently, reports on bifunctional acid-base catalysts<sup>11</sup>, ion-exchange

resin<sup>12</sup>, double metal cyanides<sup>13</sup>, heteropoly acid/zirconia<sup>14</sup>, amberlyst<sup>15</sup>, basic zeolite<sup>16</sup>, supported metal hydroxides<sup>17</sup>, mixed metal oxides<sup>18</sup> are available. Spinel catalysts are metal oxide or catalyst support with applications in various chemical processes due to high mechanical, chemical, and thermal stability and porous structure. For the transesterification reactions, the catalyst with a wide pore value is required for the triglyceride molecules to diffuse and react. Sankaranarayanan *et al.*<sup>19</sup> have investigated mixed oxide AB<sub>2</sub>O<sub>4</sub> (A=Co, Ni, Cu, and Zn and B = Al, Fe, and Co) catalyst for transesterification of vegetable oils and found that Zn-containing spinels are relatively active. The activity is correlated with the A ion's ease of polarisation.

Contrary to conventional heating for biodiesel production, microwave-assisted transesterification reactions are promising due to their rapid heating, energy efficiency, short residence time, cost-saving, and environmental friendliness. In the presence of microwaves, hotspots that act as active sites for catalytic activity improve the conversion rate and efficiency along with the reduction in heat input. By-product formation is relatively less and thus simplifies the downstream processing<sup>20</sup>. We report the utilization of zinc ferrite (ZnFe<sub>2</sub>O<sub>4</sub>) material prepared using the sol-gel method as the catalyst for the transesterification reaction of WCO and further its characterization. Transesterification reactions under microwave conditions can improve reaction performance due to improved heating and, thus, facilitating biodiesel production in mild conditions.

## Experimental Section

### Catalyst synthesis and characterization

Zinc ferrite (ZnFe<sub>2</sub>O<sub>4</sub>) spinel nanomaterial was synthesised using the sol-gel method. Zinc sulphate (ZnSO<sub>4</sub>·H<sub>2</sub>O), ferrous/iron sulphate (FeSO<sub>4</sub>·7H<sub>2</sub>O), citric acid, and ammonium hydroxide solution were used for the preparation. A stoichiometric quantity of metal precursor of zinc sulphate and iron sulphate pre-mixed and dissolved in distilled water were added together under stirring. After mixing, citric acid was added by maintaining the metal: citric acid molar ratio of 1:1.5. To keep the pH at 9, ammonium hydroxide solution was added drop by drop. Then the solution was further heated under the stirring conditions at 80°C temperature until the gel formation. Further, the obtained gel was transferred to the hot air oven at 150°C for 12 h to obtain the black precursor. The final

sample was calcined at 600°C for a period of 4 h in a muffle furnace.

The metal oxide obtained from the sol-gel process was further characterized using x-ray diffraction (XRD) and scanning electron microscope-energy dispersive x-ray spectroscopy (SEM-EDS). XRD analysis was performed using a Panalytical X-pert powder diffractometer with a Cu K $\alpha$  radiation source, Cu target X-Ray tube, operated at 2 kW x-ray power, 2 $\theta$  range of 20-80°, and 0.02 step size. The Debye-Scherrer equation and Bragg's equation were used to calculate the average crystallite size and lattice parameter, respectively. SEM-EDS analysis was conducted using a TESCAN VEGA3 LMU of 15 kV HV to obtain a surface image and composition of the nanomaterial.

### Biodiesel manufacturing from Waste Cooking Oil (WCO)

WCO was procured from the local restaurants near Warangal, Telangana. Initially, the oil was cleaned by filtration to remove the solid impurities, dried, and stored. The acid value of WCO was calculated around <3 mg KOH/g for the feedstock; thus, it was directly used for the transesterification reaction. A fixed amount of WCO was mixed completely with ZnFe<sub>2</sub>O<sub>4</sub> catalyst and ethanol in a three-neck flask. The three-neck flask was then placed in the microwave-assisted reactor setup (NUWAV-UNO) along with the condenser setup to collect the vapour. Reactions were conducted under different conditions of catalyst loading in the range of 4-8 wt%, ethanol:oil volume ratio in the range of 3:1-9:1, the reaction temperature in the range of 40-60°C, and reaction time of 10-20 min under fixed microwave power of 200 W and stirring speed of 800 rpm. After the reaction, unreacted ethanol was separated from the biodiesel layer in a separating funnel, and the catalyst was isolated from the product using filtration. The reactor setup used for the transesterification reaction is shown in Fig. 1. The catalyst reusability was tested by adopting the same reaction conditions and reusing the isolated catalyst from the previous cycle to the next cycle without any treatment.

The biodiesel yield from the transesterification reaction was estimated using the formula in Eq. (1).

$$\text{Biodiesel yield (\%)} = \frac{\text{Weight of Biodiesel obtained}}{\text{Weight of WCO}} \times 100 \quad \dots(1)$$

Physiochemical properties of both WCO and biodiesel were calculated, including density,



Fig. 1 — Microwave-assisted transesterification reaction setup

kinematic viscosity at 40°C using Ostwald viscometer, and acid value by ASTM D664 method. The Pensky-Martens apparatus with closed cup method was used to analyse the flash point and fire point of the sample. Fourier Transform Infra-Red (FTIR) spectroscopy of biodiesel and WCO was tested using a Perkin Elmer 100S FTIR spectrophotometer. The infrared absorption spectra were performed in the medium infrared range of 800-2000  $\text{cm}^{-1}$ .  $^1\text{H-NMR}$  analysis of the biodiesel sample was conducted using a Bruker Ascend 400 MHz spectrometer under ambient temperature conditions. About 50 mg of biodiesel was combined with 0.7 mL of deuterated chloroform ( $\text{CDCl}_3$ ) solvent and 0.05% TMS and further analysed to obtain  $^1\text{H-NMR}$  spectra.

## Result and Discussion

### Catalyst characterization

#### X-ray diffraction (XRD)

The XRD pattern of zinc ferrite ( $\text{ZnFe}_2\text{O}_4$ ) spinel nanomaterial is shown in Fig. 2. The XRD pattern showed the crystalline nature, spinel-type structure with space group  $Fd\bar{3}m$ , and pure phase without any impurities or single phase of zinc or iron oxide. Based on the XRD data, the peak at  $2\theta = 29.9^\circ, 35.3^\circ, 42.9^\circ, 53.2^\circ, 56.7^\circ, 62.2^\circ,$  and  $73.5^\circ$  were indexed to (220), (311), (400), (422), (511), (440), and (533) that matches with the literature (JCPDS 82-1049)<sup>19,21</sup>. For the sharp (311) peak of the  $\text{ZnFe}_2\text{O}_4$  sample, the Scherrer equation determined the crystallite size to be 43.68 nm and the average crystallite size as 37.96 nm. The XRD plot and crystallite size value confirmed the high degree of crystallinity of spinel nanoparticles.

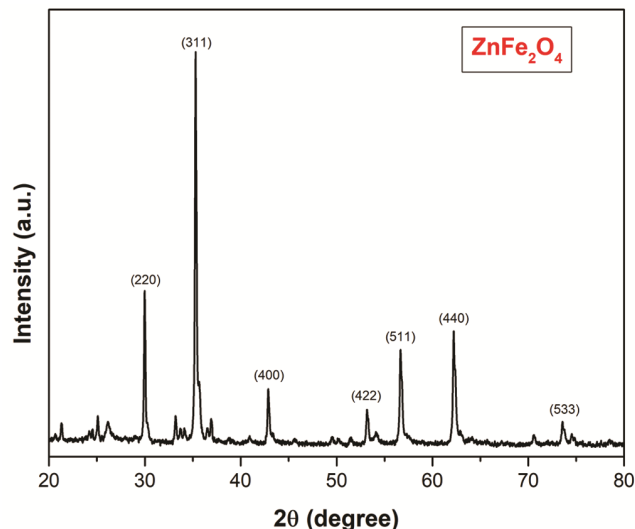


Fig. 2 — X-ray diffractogram of  $\text{ZnFe}_2\text{O}_4$  nanomaterial

The interplanar distance,  $d$ , calculated by Bragg's equation for intense (311) peak was around 2.98 Å. The average crystallite size, interplanar distance, and lattice constant calculated for the  $\text{ZnFe}_2\text{O}_4$  sample are tabulated in Table 1 and compared with the literature data that confirms the spinel nanostructure formation in the current study.

#### Scanning electron microscope (SEM)

The SEM images of  $\text{ZnFe}_2\text{O}_4$  spinel nanomaterial are given in Figs 3(a) and 3(b) at different points. The images confirm that the particles were arranged densely with uniform nanoparticles of almost spherical shape and agglomerated to form larger particles. The elemental composition calculated by averaging EDS at various positions accounts for Zn of 13% and Fe of 19%, approximately the same as the experimental values. The EDS image corresponding to Fig. 3(c) is given in Fig. 3(d). The synthesised  $\text{ZnFe}_2\text{O}_4$  spinel nanomaterial was further tested as the catalyst for WCO transesterification to produce biodiesel.

#### Reaction parameter effect

##### Time of reaction

The change in the yield of biodiesel with respect to the change in reaction time between 10 to 20 min by fixing other variables is shown in Fig. 4. Table 2 lists the yield of the biodiesel obtained by varying different parameters. The maximum biodiesel yield of 94.7 % was observed at 15 min reaction time. When the time was reduced to 10 min, the biodiesel yield was around 62.7 %, and when the time increased to 20 min, the yield was around 83.9 %. Low yield under

Sample	Synthesis method	Average crystallite size, D (nm)	Interplanar distance, d (Å)	Lattice parameter, a (Å)	Reference
ZnFe <sub>2</sub> O <sub>4</sub>	Sol-gel method calcined at 600°C/4h	37.9	2.98	8.42	This work
ZnFe <sub>2</sub> O <sub>4</sub>	Co-precipitation method calcined at 600°C/6h	32	--	8.415	[19]
ZnFe <sub>2</sub> O <sub>4</sub>	Thermal decomposition refluxed at 290°C/2 h	9.8	2.52	8.411	[21]

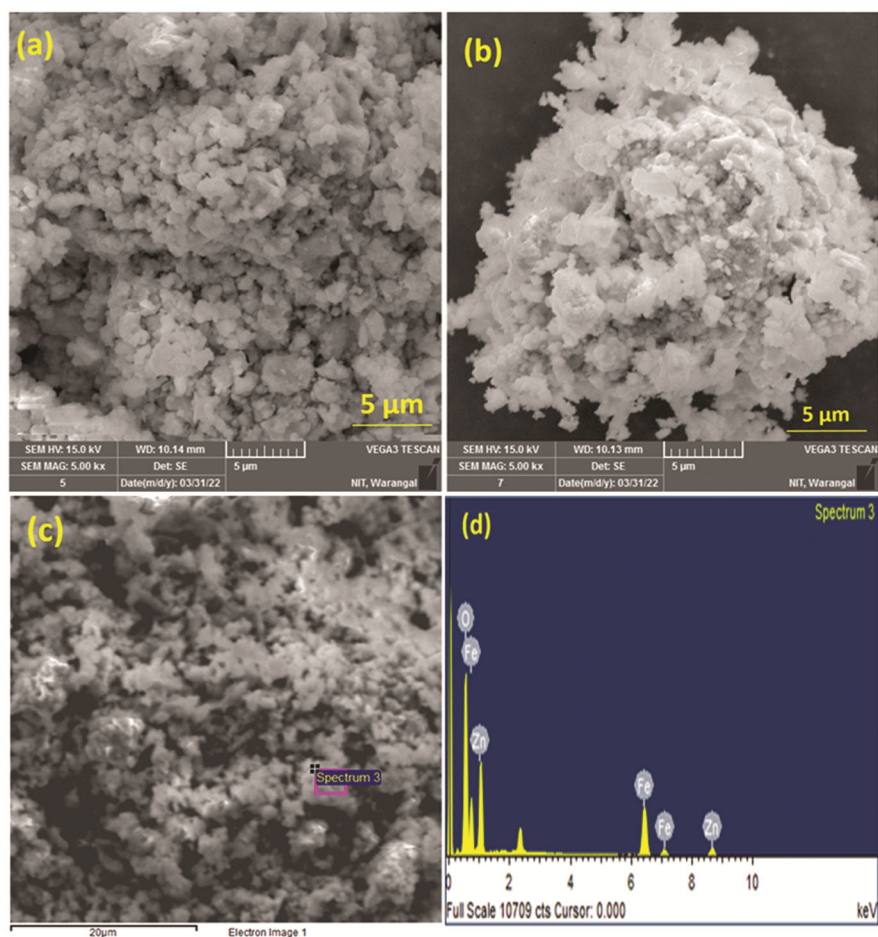


Fig. 3 — (a) and (b) The SEM image of ZnFe<sub>2</sub>O<sub>4</sub> nanomaterial, (c) SEM image from which EDS data is obtained and (d) EDS image of the sample

short reaction time is due to an incomplete transesterification reaction that results in unreacted triglycerides. The longer reaction time may improve the reverse reaction progress and thus reduce the concentration of triglycerides<sup>5</sup>.

#### Temperature of reaction

The correlation of reaction temperature on biodiesel yield for a 40-60°C temperature range at the reaction time of 15 min, catalyst loading of 6 wt%, and ethanol:oil ratio of 6:1 is given in Fig. 5. The maximum

yield of 94.7% was obtained at a temperature of 50°C; at lower temperature of 40°C the yield was also low at 83.3%, and at higher temperature of 60°C the yield has reduced to 83%. If the reaction temperature is too low, the conversion of triglyceride to biodiesel may not be efficiently complete due to the non-availability of sufficient energy to overcome the energy barrier. When the temperature has raised to 60°C the methylation reaction may be affected since the portion of ethanol gets evaporated and cannot effectively participate in the transesterification reaction<sup>22</sup>.

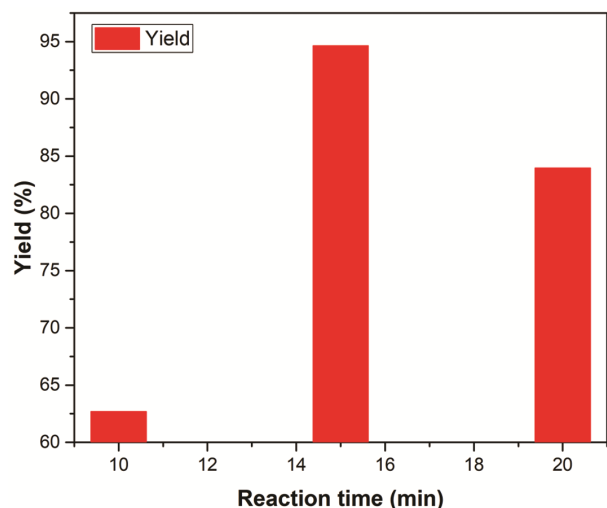


Fig. 4 — Time vs biodiesel yield at constant temperature of 50°C, catalyst loading of 6 wt % and ethanol:oil ratio of 6:1

Table 2 — Yield of biodiesel obtained based on experimental study by varying different parameters

Run	Time (min)	Temp °C	Catalyst (% wt)	Ethanol : oil	Actual Yield (%)
1.	15	50	6	3	80.8
2.	15	50	6	6	94.66
3.	15	50	6	9	79.21
4.	15	50	4	6	82.83
5.	15	50	6	6	94.66
6.	15	50	8	6	73.68
7.	15	40	6	6	83.31
8.	15	50	6	6	94.66
9.	15	60	6	6	83
10.	10	50	6	6	62.7
11.	20	50	6	6	83.98
12.	15	50	6	6	94.66

#### Catalyst loading

The catalyst quantity influence on the yield of the product was analysed by changing the catalyst concentration between 4-8 wt % at a constant reaction time of 15 min, reaction temperature of 50°C, and ethanol:oil ratio of 6:1. The trend in yield is shown in Fig. 6 with respect to change in catalyst loading. When the catalyst loading was 4 wt%, the biodiesel yield was around 82.8%. As the weight of the catalyst increased to 6 wt%, the yield improved to 94.7%; however, further increasing the weight reduced the yield to 73.7%. With the catalyst overdose, the saponification reaction increases, thus reducing the biodiesel yield<sup>5</sup>.

#### Ethanol:oil ratio

By varying the ethanol:oil ratio in the range of 3:1 to 9:1, the biodiesel yield was analysed under a

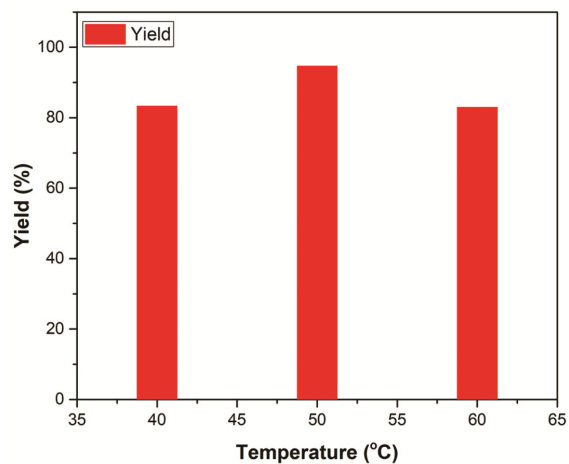


Fig. 5 — Temperature vs biodiesel yield at constant time of 15 min, catalyst loading of 6 wt % and ethanol:oil ratio of 6:1

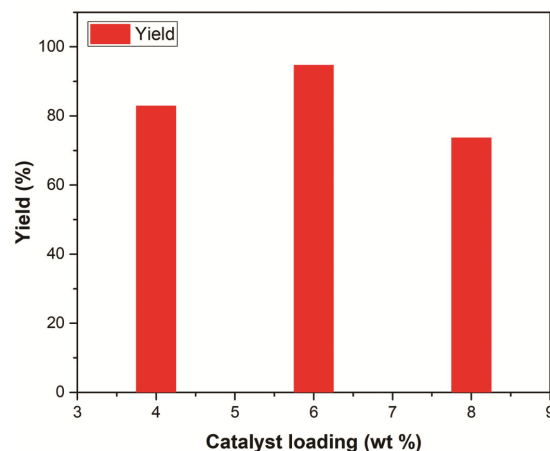


Fig. 6 — Catalyst loading vs biodiesel yield at constant time of 15 min, temperature of 50°C, and ethanol:oil ratio of 6:1

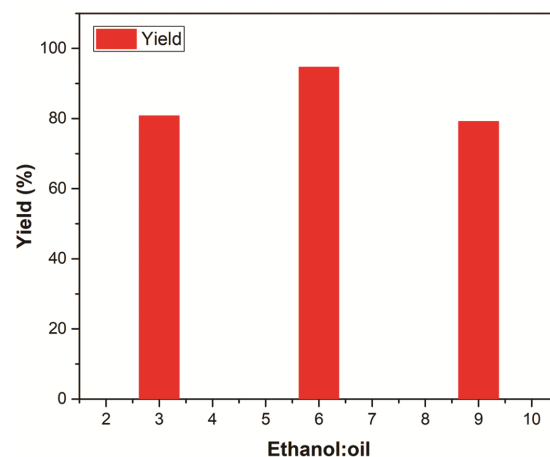


Fig. 7 — Ethanol:oil vs biodiesel yield at constant time of 15 min, temperature of 50°C, and catalyst loading of 6 wt %

constant reaction time of 15 min, reaction temperature of 50°C, and catalyst loading of 6 wt % and the trend is shown in Fig. 7. The optimized ethanol:oil ratio

was 6:1, which resulted in maximum yield. For ethanol: oil ratio of 3:1, the yield was around 80.8 %, and when the ratio increased to 9:1, the biodiesel yield was around 79.2%. At least 6 mol of alcohol is required for 1 mol of triglyceride since transesterification is a reversible reaction and alcohol evaporates, which requires more content for better conversion. As the ethanol concentration is increased, the glycerol solubility in alcohol leads to an emulsification reaction that reduces the yield of biodiesel<sup>5</sup>. Overall, an optimum reaction time, reaction temperature, catalyst loading, and ethanol:oil molar ratio should be maintained to favour the proper contact between oil and alcohol to react effectively.

#### Waste cooking oil and biodiesel characterization

The biodiesel was successfully developed by transesterification reaction of WCO using the spinel catalyst. The properties of the WCO and biodiesel obtained by the transesterification reaction of WCO is shown in Table 3, along with the ASTM standard. The formation of biodiesel was verified by the

Table 3 — Properties of WCO and biodiesel obtained in this work

	WCO	Biodiesel	ASTM-6751 biodiesel
Kinematic viscosity at 40°C (cP)	3.62	4.1	1.9-6.0
Acid value (mg KOH/g oil)	2.45	1.61	<0.8
Density (g/m <sup>3</sup> )	0.876	0.864	0.86-0.90
Flash point (°C)		150	100-170
Fire point (°C)		160	

properties of the fuel, which are in agreement with those documented in the literature. Table 4 compares the properties of the biodiesel, diesel fuel and WCO obtained in this work with those in the literature reported<sup>20</sup>. FTIR and NMR analyses are discussed in more detail to validate the functional group presence and other molecules in biodiesel.

#### Fourier transform infrared (FT-IR) spectroscopy

The FTIR spectra of WCO and the biodiesel produced from WCO using ZnFe<sub>2</sub>O<sub>4</sub> catalyst with yield of 94.66%, 94.20%, 86.66%, and 84.75% are shown in Fig. 8(a). The peak position remains consistent with all the samples. However, the peak intensity varies for each sample. The peak at 722 cm<sup>-1</sup> matches the out-of-plane bending of the CH<sub>2</sub> molecule; 1160 cm<sup>-1</sup> peak indicates O-CH<sub>3</sub> stretching vibration, 1377 cm<sup>-1</sup> indicates the absorbance by the -CH<sub>3</sub> bond, 1462 cm<sup>-1</sup> peak represents CH<sub>3</sub> asymmetric bending, 1746 cm<sup>-1</sup> corresponds to C=O stretching band of methyl ester. The aliphatic-H is indicated by peaks at 2854 cm<sup>-1</sup> and 2925 cm<sup>-1</sup>. The peak at 3008 cm<sup>-1</sup> indicates HC=CH bond association<sup>23,24</sup>. Specifically, the IR band at 1160 cm<sup>-1</sup>, 1462 cm<sup>-1</sup>, and 1746 cm<sup>-1</sup> corresponds to the peak for biodiesel. The variation in these two peak intensities for biodiesel of different yields with respect to WCO is evident in Figs 8(b) and 8(c), respectively. Biodiesel formation well confirmed from the analysis.

Table 4 — Comparison of the biodiesel and waste cooking oil properties

Sample	Acid value (mg KOH/g oil)	Specific density	Kinematic viscosity at 40°C	Flash Point (°C)	Fire point (°C)	Reference
ASTM D6751	<0.5	0.87-0.89	1.9-6	>93	--	[17]
Diesel fuel	0.24	0.846	2.28	68	--	
Waste cooking oil	0.34	0.87-0.88	2.25-3.10	--	--	
Biodiesel BIS 15607:2016	0.5	0.86-0.9	3.5-5.0	101	--	[23]
WCO	2.45	0.92	3.62	--	--	This work
Biodiesel	1.61	0.864	4.1	150	160	

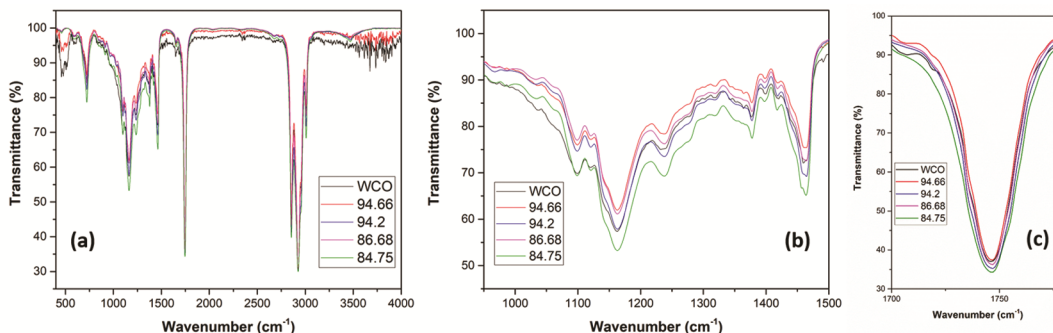


Fig. 8 — FTIR spectra of WCO and biodiesel at different yield (a) over full range, (b) in the range 900-1500 cm<sup>-1</sup>, and (c) in the range 1700-1780 cm<sup>-1</sup>

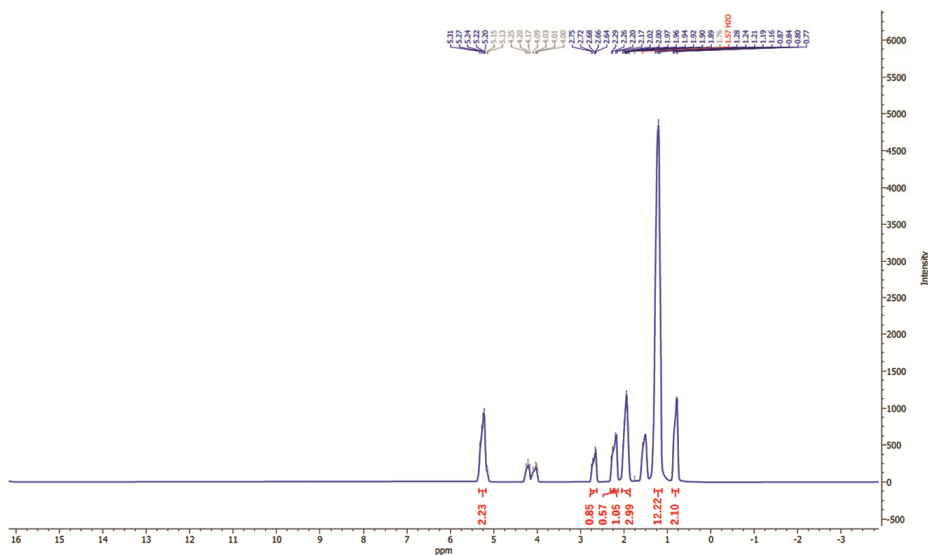
Fig. 9 —  $^1\text{H-NMR}$  analysis of biodiesel sample

Table 5 — Yield of biodiesel for reusability of the catalyst

Run No.	Time (min)	Temp ( $^{\circ}\text{C}$ )	Catalyst weight (%)	Ethanol: Oil	Yield post reusability experiments (%)
1.	15	50	3	6:1	94.66
2.	15	50	3	6:1	90.44
3.	15	50	3	6:1	89.50
4.	15	50	3	6:1	80.95

#### Nuclear magnetic resonance (NMR) spectroscopy

The  $^1\text{H-NMR}$  analysis of WCO and biodiesel produced from WCO is shown in Fig. 9. The peak at 0.85 ppm is the characteristic of triglyceride ( $-\text{CH}_3$ ) terminals present in saturated or unsaturated fatty acid chains, the sharp signal at 1.25 ppm corresponds to methylene group ( $-\text{CH}_2-$ ) of long fatty acid, 1.5 ppm represents carbonyl methylene group, 1.9 ppm signal represents  $-\text{CH}_2-$  adjacent to double bonds, multiplet at 2.2 ppm correlates to the  $-\text{CH}_2-$  present adjacent to the carbonyl group, 2.7 ppm represents a bisallylic group of unsaturated fatty acid, signals at 4.15–4.3 ppm attributes to the proton of glyceride  $-\text{CH}_2$  functionality and signal at 5.2 was due to the olefinic carbon ( $-\text{CH}=\text{CH}-$ ). The formation of biodiesel can be assured by the presence of the carbonyl groups at the chemical shift of 2.2 ppm in the samples<sup>25</sup>.

#### Catalyst reusability

The  $\text{ZnFe}_2\text{O}_4$  spinel catalyst used for the transesterification reaction was filtered from the liquid solution obtained from the transesterification reaction under optimized conditions and further used as the catalyst for the next cycle to test the recyclability of the catalyst. The yield obtained in each run is listed in Table 5. Fig. 10 shows the biodiesel yield from the

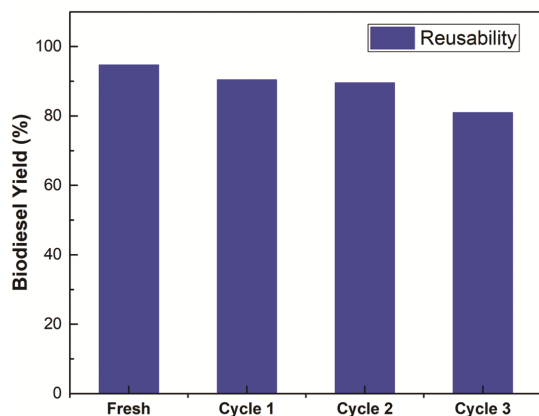


Fig. 10 — Reusability test of the catalyst for multiple cycle under optimized reaction condition

transesterification reaction after repeated catalyst usage for multiple cycles. The yield has reduced from 94.7% for the fresh catalyst to 80.9% in the third cycle. Around 14% drop in active site on the catalyst surface can be observed after repeated usage for 3 cycles, which aligns with the reported values<sup>26</sup>. The degradation in the active sites is reported to be caused by active site blockage, deterioration in the active sites, and leaching of active sites.

#### Microwave reaction mechanism

The efficient heating of the reaction mixture during the transesterification reaction using microwave irradiation ensures an increased reaction rate with lesser side product formation. The electromagnetic energy in the microwave is transferred into heat energy using the liquid components present in the reaction mixture. The interaction of microwaves with

the materials can form electric and magnetic fields, which are responsible for dielectric heating and magnetic loss heating, respectively<sup>20</sup>. The ferrite materials have been reported to show magnetic heating of approximately four times higher than dielectric loss, corresponding to a higher catalyst heating rate using the microwave over conventional electric heating<sup>27</sup>.

### Conclusion

The ZnFe<sub>2</sub>O<sub>4</sub> spinel nanomaterial was synthesised by the sol-gel synthesis method, and the XRD characterization confirmed the *Fd $\bar{3}$ m* space group with an average crystallite size of 37.96 nm. Furthermore, the developed ZnFe<sub>2</sub>O<sub>4</sub> spinel nanomaterial was adopted as the catalyst for waste cooking oil (WCO) transesterification reaction under a microwave environment for biodiesel formation. The effect of reaction parameters were analyzed, and it was found that the optimized conditions were a 15 min reaction time, 50°C reaction temperature, 6 wt% catalyst, and 6:1 ethanol:oil ratio, respectively, yielding a maximum biodiesel of 94.7%. FTIR analysis of WCO and biodiesel confirmed the various functional groups in the samples, and the formation of biodiesel was validated by <sup>1</sup>H-NMR analysis. The reusability study confirmed that a biodiesel yield of around 80.9% was obtained when the catalyst from the initial cycle was reused for 3 cycles under the same reaction conditions.

### Acknowledgments

Research Seed Money, National Institute of Technology, Warangal (P1120-Plan-Gen.RSM- Dr. Anjana PA) has funded this work. The authors acknowledge the support by Central Research Instrumentation Facility (CRIF), National Institute of Technology, Warangal for the analysis of XRD, SEM-EDS, and NMR. Also, we thank Department of Chemistry, National Institute of Technology, Warangal for FTIR analysis.

### References

- 1 Countries O of the PE, OPEC monthly oil market report feature article: Assessment of the global economy (2024).
- 2 International energy agency, net zero by 2050: A roadmap for the global energy sector, (2021).
- 3 Zik N, Sulaiman S & Jamal P, Biodiesel production from waste cooking oil using calcium oxide / nanocrystal cellulose / polyvinyl alcohol catalyst in a packed bed reactor, *Renew Energy*, 155 (2020) 267.
- 4 Milano J, Ong H C, Masjuki H H, Silitonga A S, Wei-Hsin C, Kusumo F, Dharma S & Sebayang A H, Optimization of biodiesel production by microwave irradiation-assisted transesterification for waste cooking oil-Calophyllum inophyllum oil via response surface methodology, *Energy Convers Manag*, 158 (2018) 400.
- 5 Hong I K, Jeon H, Kim H & Lee S B, Preparation of waste cooking oil based biodiesel using microwave irradiation energy, *J Ind Eng Chem*, 42 (2016) 107.
- 6 Rabia S N R, Devi K S & Kumar M N, Modified *Malleus malleus* shells for biodiesel production from waste cooking oil: An optimization study using Box-behnken design, *Waste Biomass Valori*, 11 (2020) 793.
- 7 Anastopoulos G, Zannikou Y, Stournas S & Kalligeros S, Transesterification of vegetable oils with ethanol and characterization of the key fuel properties of ethyl esters, *Energies*, 2 (2009) 362.
- 8 Kiss F E, Jovanović M & Bošković G C, Economic and ecological aspects of biodiesel production over homogeneous and heterogeneous catalysts, *Fuel Process Technol*, 91 (2010) 1316.
- 9 Dalvand P & Mahdavian L, Biodiesel production in the presence of eggshell nano-catalyst, *Chem Technol Fuels Oils*, 58 (2022) 55.
- 10 Acosta P I, Campedelli R R, Correa E L, Bazani H A G, Nishida E N, Souza B S & Mora J R, Efficient production of biodiesel by using a highly active calcium oxide prepared in presence of pectin as heterogeneous catalyst, *Fuel*, 271 (2020) 117651.
- 11 Dai Y M, Li Y Y, Lin J H, Chen B Y & Chen C C, One-pot synthesis of acid-base bifunctional catalysts for biodiesel production, *J Environ Manag*, 299 (2021) 113592.
- 12 Patiño Y, Faba L, Díaz E & Ordóñez S, Biodiesel production from wastewater sludge using exchange resins as heterogeneous acid catalyst: Catalyst selection and sludge pre-treatments, *J Water Process Eng*, 44 (2021) 102335.
- 13 Yan F, Yuan Z H, Lü P M, Luo W, Yang L M & Deng L, Synthesis of biodiesel by Fe(II)-Zn double-metal cyanide complexes, *J Fuel Chem Technol*, 38 (2010) 281.
- 14 Alcañiz-Monge J, El-Bakkali B, Trautwein G & Reinoso S, Zirconia-supported tungstophosphoric heteropolyacid as heterogeneous acid catalyst for biodiesel production, *Appl Catal B Environ*, 224 (2018) 194.
- 15 Ilgen O, Akin A N & Boz N, Investigation of biodiesel production from canola oil using Amberlyst-26 as a catalyst, *Turkish J Chem*, 33 (2009) 289.
- 16 Al-Ani A, Mordvinova N E, Lebedev O I & Khodakov A Y, Ion-exchanged zeolite P as a nanostructured catalyst for biodiesel production, *Energy Rep*, 5 (2019) 357.
- 17 Buasri A, Chaikut N, Loryuenyong V, Rodklum C, Chaikwan T & Kumphan N, Continuous process for biodiesel production in packed bed reactor from waste frying oil using potassium hydroxide supported on *Jatropha curcas* fruit shell as solid catalyst, *Appl Sci*, 2 (2012) 641.
- 18 Kumar V, Kasimani R & Subramanian D, Production of biodiesel from tannery waste using a stable and recyclable nano-catalyst: An optimization and kinetic study, *Fuel*, 260 (2020) 116373.
- 19 Sankaranarayanan T M, Shanthi R V, Thirunavukkarasu K, Pandurangan A & Sivasanker S, Catalytic properties of spinel-type mixed oxides in transesterification of vegetable oils, *J Mol Catal A: Chem*, 379 (2013) 234.
- 20 Nomanbhay S & Ong M Y, A review of microwave-assisted reactions for biodiesel production, *Bioengineering*, 4 (2017) 2.

- 21 Guo X, Zhu H, Si M, Jiang C, Xue D, Zhang Z & Li Q, ZnFe<sub>2</sub>O<sub>4</sub> nanotubes: Microstructure and magnetic properties, *J Phys Chem C*, 118 (2014) 30145.
- 22 Aghbashlo M, Hosseinpour S, Tabatabaei M & Mojarab S M, Multi-objective exergetic and technical optimization of a piezoelectric ultrasonic reactor applied to synthesize biodiesel from waste cooking oil (WCO) using soft computing techniques, *Fuel*, 235 (2019) 100.
- 23 Mahamuni N N & Adewuyi Y G, Fourier transform infrared spectroscopy method to monitor soy biodiesel and soybean oil in transesterification reactions, petrodiesel- biodiesel blends, and blend adulteration with soy oil, *Energy Fuels*, 23 (2009) 3773.
- 24 Mumtaz M W, Adnan A, Anwar F, Mukhtar H, Raza M A, Ahmad F & Rashid U, Response surface methodology: An emphatic tool for optimized biodiesel production using rice bran and sunflower oils, *Energies*, 5 (2012) 3307.
- 25 Doudin K I, Quantitative and qualitative analysis of biodiesel by NMR spectroscopic methods, *Fuel*, 284 (2021) 119114.
- 26 Li H, Wang Y, Ma X, Wu Z, Cui P, Lu W, Liu F, Chu H & Wang Y, A novel magnetic CaO-based catalyst synthesis and characterization: Enhancing the catalytic activity and stability of CaO for biodiesel production, *Chem Eng J*, 391 (2020) 123549.
- 27 Zhiwei P, Jiann-Yang H & Matthew A, Magnetic loss in microwave heating, *Appl Phys Express*, 5 (2012) 027304.